SCIMMS

Simulated Chromatography of Interactive MacroMolecular Systems

DRAFT: 08-30-93

F.J. Stevens

Center for Mechanistic Biology and Biotechnology

Argonne National Laboratory

Introduction

The interactions of two or more macromolecules, such as occur in the binding of antigen by antibody or protein binding to nucleic acids , result in the formation of a complex having larger Stokes' radius than its constituents. Because size-exclusion chromatography, to a first approximation, separates molecules on the basis of differences in Stokes' radii, the application of size-exclusion chromatography for the detection and characterization of such interactions has been long recognized. A partial listing of publications describing various methods and objectives of its utility include: Hummel & Dryer, 1962; Andrews, 1964; Ackers & Thompson, 1965; Dishon *et al*, 1966; Sullivan & Riggs, 1967; Ackers, 1975; Cox, 1978; Cann & Hinman,1976; Stevens *et al*, 1980; Cox & Dale, 1981; Dickerman *et al*, 1981; Stevens & Schiffer, 1981; Endo *et al*., 1982; Endo & Wada, 1983; Stevens, 1986; Stevens *et al*, 1986; Cann & Winzor, 1987; Cann *et al*, 1988; Cann *et al*, 1989; Myatt *et al*, 1989; Stevens, 1989, Myatt *et al*,1991.

The high speed and precision found with contemporary chromatography technologies, coupled with routine use of digital data collection, motivate the development of simulations which can extract information regarding the affinity, kinetic, and specificity properties of macromolecules from the shape and concentration dependence of size-exclusion chromatograms. Because size-exclusion chromatography is a technique that reveals the most general consequence of macromolecular interaction; *i.e.*, changes in Stokes' radius, the availability of a rigorous and convenient means to interpret chromatography results could have broad application.

SCIMMS (Simulated Chromatography of Interactive MacroMolecular Systems) represents our current simulation effort to provide a tool that may provide some assistance for both qualitative and quantitative interpretation of the elution profiles exhibited by interacting molecules. As presently developed, SCIMMS may be used to simulate (1) self-association (homologous association) of monomers to form dimers, (2) higher-order aggregation of dimers to form polymers, (3) heterologous association of two molecules of equal or unequal molecular weights, (4) heterologous competitive association of three molecules of equal or unequal molecular weights. The algorithm may be used to emulate small-zone or large-zone configurations in addition to permitting the column to be saturated with one of the reaction components. In this document, we review the theoretical basis for the algorithm and illustrate its application.

Purpose of the simulation. SCIMMS is the result of intermittent software development effort prompted by changing research activities in our laboratory. The original simulation (Stevens et al, 1980; Stevens & Schiffer, 1981) was a tool to help understand the diversity of size-exclusion chromatography patterns found during purification of human antibody light chains (Bence Jones proteins) prior to crystallization attempts. Samples obtained from different patients were found to consist of covalent dimers and free monomers of the expected molecular weights when analyzed electrophoretically. However, the patterns observed by chromatography contradicted the electrophoretic results.

Although the covalent dimer component of the sample was usually found to elute at the position expected for a globular protein of its molecular weight, the monomeric components from different patients were found at positions corresponding to monomers, dimers, or proteins of intermediate molecular weight. Elution profiles at intermediate positons were found to be asymmetric.

It was known that light chains were capable of forming non-covalent dimers. It was not anticipated that this capability would influence chromatography behavior, or that light chains obtained from different patients could behave in strikingly different manners. To explore the hypothesis that different chromatography patterns resulted from differences in affinity of dimerization, a simple simulation basically consisting of alternating iterations of equilibration and transport of monomers and dimers was developed. The simulation indicated that the variation in elution profiles that was observed for the Bence Jones proteins was consistent with variations in affinity of dimerization that ranged over at least three orders of magnitude. The asymmetry of elution profile for proteins eluting at positions intermediate between monomer and dimer was satisfactorily replicated.

The experiments involving Bence Jones proteins were performed on a preparative basis at flow rates that generated one run per day. With the advent of high performance chromatography with much shorter run times and computerized data collection, it became reasonable to consider analytical scale size-exclusion chromatography as a means for more general analysis of macromolecular interactions, such as the binding of antigen by monoclonal antibody.

A new simulation was developed that allowed fractional constituent velocities as opposed to integer velocities employed in the original simulation. The initial scheme, which required that column size be scaled to accomodate different elution velocities of constituent molecules, had been acceptable in the specialized case of monomer–dimer interconversion. Fractional velocities were incorporated by introducing a gaussian representation of transport, in which the elution velocity was considered to be the mean displacement of solute per iteration cycle, and the standard deviation was considered to represent dispersion of sample during each transport cycle. This simulation also incorporated the possibility of bivalent interactions, which required the determination of unbound, singly-bound, and doubly-bound fractions of the bivalent component (Stevens, 1986).

The first and second generation simulations calculated changes in concentration of free and bound compenents by assuming equilibration during each transport cycle. In retrospect, this assumption was probably reasonable for the original Bence Jones protein studies which involved long run times and relatively low affinity interactions. However, for analytical mode (HPLC) experiments requiring 15 - 30 minutes, each iteration cycle represents a period of only a few seconds, insufficient for equilibration of moderate to high affinity interactions.

This issue was addressed in a simulation in which forward and reverse rate constants were considered as probabilities of (multiple) association and dissociation events during the iteration time element (Stevens, 1989). The simulation demonstrated that kinetic properties are significant determinants of elution profile during run times characteristic of analytical mode chromatography and accurately reproduced kinetically controlled boundary profiles of large zone chromatography.

The current fourth generation simulation (tentatively identified as SCIMMS) combines, for the first time, the capabilities of the previous more specialized algorithms. It can be used in conjunction with self-association studies as well as monovalent or bivalent heterologous interaction experiments. Kinetic control of interactions is implicitly incorporated although the stochastic formulation described above has been eliminated on the basis that contemporary computing resources allow the use of sufficiently small time steps to avoid the concern for multiple association-dissociation events.

Current research interests in this laboratory address the issue of higher order aggregation of Bence Jones proteins. This phenomenon had been noted in the original study of light chain dimerization (Stevens *et al*, 1980) but was not understood. More recently, we have found that the propensity of antibody light chains to form high molecular weight complexes correlates with the finding of tissue deposition in the multiple myeloma patient who produced the protein (Stevens et al, 1991). Therefore, SCIMMS incorporates a model of aggregation in which dimers formed by homologous association can further aggregate to form multi-subunit oligomers. By reducing the concentration of free protomer, interaction with another constituent inhibits oligmerization and provides a mechanism to emulate drug antagonism of aggregation.

Future algorithm development, if warranted, may include incorporation of a mechanism to inhibit oligomerization at the level of dimer–dimer interaction, bivalent interactions involving two non-identical sites, and implementation of a more physically realistic representation of the solute transport process. This new transport algorithm is expected to better reflect the consequences of physical separation of potentially interacting molecules by the porous chromatography matrix.

Background

Noncovalent interaction between molecule A and molecule B results in the production of complex C having larger Stokes' radius than either A or B. If A and B do not interact then, in principle, a chromatogram of a mixture of A and B will be equivalent to an arithmetic summation of chromatograms of A and B run separately. Differences between the experimental chromatogram of the mixture, and the combined chromatograms of the separate constituents reveals interaction between A and B. The magnitude and shape of the chromatographic variation are determined by the affinity and kinetics of interaction. Homologous interactions; *i.e.*, self-association, are revealed as concentration-dependence of the elution profile.

Equilibrium expressions. The equilibrium concentrations of A, B, and C are given by

$$c = \mathrm{K}ab \qquad (1)$$

where a, b, and c are molar concentrations and K is the equilibrium (association) constant. Substituting $a = a_0 - c$ and $b = b_0 - c$, the equilibrium concentration c can be related to the initial concentrations of A and B as

$$c = \lambda - (\lambda^2 - a_o b_o)^{1/2} \qquad (2)$$

where $\lambda = (a_o + b_o + K^{-1}) / 2$. (3)

In the special case of homologous interaction to form dimers, the equilibrium equation becomes

$$c = Ka^2 \qquad (4)$$

Substituting $a = a_0 - 2c$ again yields a similar expression for c

$$c = \lambda - (\lambda^2 - (a_o/2)^2)^{1/2} \qquad (5)$$

in which $\lambda = (a_o + (4K)^{-1}) / 2$. (5a)

Kinetic expressions. The interactions of two molecules A and B to form C are described by the equation

$$\frac{dc}{dt} = k_f\, ab - k_r\, c \qquad (6)$$

in which k_f and kr are the forward and reverse kinetic rate constants, respectively. At equilibrium, (dc/dt) = 0; therefore, the equilibrium concentration is given by

$$c = (k_f / k_r)\, ab \qquad (7)$$

Equations 1 and 7 are equivalent; therefore,

$$K = (k_f / k_r) \qquad (8)$$

Following mixing of A and B, the time-dependent concentration of C is given by

$$c(t) = c\,(1 - e^{-t/\tau}) \qquad (9)$$

Generalized, following change in concentrations, relaxation to equilibrium can be expressed as

$$c(t) = c - (c(0) - c)\, e^{-t/\tau} \qquad (10)$$

The relaxation time constant

$$\tau = [\, k_f\,(a + b) + k_r\,]^{-1} \qquad (11)$$

is a function of both rate constants as well as the equilibrium concentrations[1] of the two reactants.

Thermodynamic digression. The following short and non-rigorous discussion is not directly relevant to the use of the SCIMMS algorithm. It is included to provide reference information that addresses the thermodynamic meaning of affinity, and links it to its macromolecular structural origin. One of the principle applications of this simulation is expected to be for systematic characterization of affinity properties of molecules having similar structures.

The equilibrium constant, K, is related to the change in the Gibbs free energy that accompanies association.

$$\begin{aligned} \Delta G &= \Delta H - T\,\Delta S \\ &= -\, RT\, ln\, K \end{aligned} \qquad (12)$$

where ΔH and ΔS are the changes in enthalpy and entropy upon the formation of a complex. T is expressed in absolute temperature units (degrees Kelvin); given the relationship 1 cal = 4.184 J, the thermodynamic gas constant R has the values:

[1]It is more accurate to state that the time constant is a function of the rate constants and initial concentrations which determine the equilibrium concentrations

$$R = 8.314\ \mathrm{J\ mol^{-1}\ K^{-1}}$$
$$= 1.987\ \mathrm{cal\ mol^{-1}\ K^{-1}}$$

Rewriting (12) as

$$K = e^{-(\Delta G/RT)} \qquad (13)$$

shows that a $\Delta G = 0$ results in $K = 1\ (M^{-1})$; *i.e.*, nil free energy change upon association results in equal probabilities of association and dissociation.

One order of magnitude variation in K corresponds to ΔG of 1.4 kcal mol^{-1} Hydrogen bonds range in energy from 0.5–1.5 kcal mol^{-1} and typical salt bridges are on the order of 1.9 kcal mol^{-1}. Solvation energies of hydrophobic amino acids ranged from 1.5 to 2.4 kcal mol^{-1} according to Eisenberg & McLachlan (1986). Therefore, single amino acid substitutions introduced either intentionally through site-specific mutagenesis or fortuitously through genetic mutation, have the potential to significantly affect protein interactions. For instance, sickle cell hemoglobin arises from a glutamic acid to valine substitution in the beta chain. According to the Eisenberg scale, this substitution results in a change of solvation energy from –0.76 kcal mol^{-1} to 1.5 kcal $mole^{-1}$, a net change of 2.26 kcal $mole^{-1}$. Because there are two beta chains in the hemoglobin tetramer, this single mutation provides a free energy decrease of 4.5 kcal $mole^{-1}$ for aggregation of hemoglobin that removes the valine side chain from water. Thus, this mutation can increase the affinity of hemoglobin aggregation by more than three orders of magnitude.

Solvation Energies (kcal / mol)

	Exp	Calc		Exp	Calc
Ala	0.42	0.67	Leu	2.32	1.90
Arg	–1.37	–2.10	Lys	–1.35	–0.57
Asn	–0.82	–0.60	Met	1.68	2.40
Asp	–1.05	–1.20	Phe	2.44	2.30
Cys	1.34	0.38	Pro	0.98	1.20
Gln	–0.30	–0.22	Ser	–0.05	0.01
Glu	–0.87	–0.76	Thr	0.35	0.52
Gly	0.00	0.00	Trp	3.07	2.60
His	0.18	0.64	Tyr	1.31	1.60
Ile	2.46	1.90	Val	1.66	1.50

From Eisenberg and McLachlan, Nature 319: 199, 1986

Another contribution to free energy changes during protein-protein interaction arises from an increase in entropy as water is displaced from the surfaces of interaction. A crude estimation of this energy contribution can be obtained from considering the increase in entropy that accompanies the melting of ice. The breaking of hydrogen bonds in the ice lattice requires 1.4 kcal mol^{-1} in enthalpy (heat of fusion). Since $\Delta G = 0$ for this phase transition; *i.e.*, all of the heat added to the system is converted to entropy, the increase in entropy is give by

$$\Delta S = (\Delta H) / T = 1.4\ \text{kcal mol-1}/ 273\ K$$
$$= 5.3\ \mathrm{cal\ mol^{-1}\ K^{-1}}.$$

If we assume that on-the-order-of 100 'frozen' water molecules are displaced in a typical protein-protein interaction, such as antibody light chain dimerization, formation of a complex is accompanied by an entropy increase of

$$\Delta S = 0.5\ \mathrm{kcal\ mol^{-1}\ K^{-1}}.$$

Since typical interactions take place at room temperature or slightly higher, the above expression suggests an entropy increase of 150 kcal mol^{-1} ($K > 10^{100}$ M^{-1}), which is clearly absurd. Water molecules at the protein surface are much less 'frozen' than those in ice and the net increase in entropy upon displacement from the protein is much less. However, it is clear that even if the gain in entropy is only 1% of that estimated, this is sufficient to account for one order of magnitude of interaction affinity.

Assuming no covalent bonds are broken in a reversible macromolecular interaction, enthalpy effects arise from Van der Walls interactions, hydrogen bond formation/breakage and ionic interactions. The amount of heat (enthalpy) required to change the temperature (kinetic energy) of a system by one degree is the heat capacity, therefore the heat capacity Cp is defined as

$$C_p = \delta H / \delta T$$

If Cp changes with temperature, this implies that the amount of heat needed to increment the vibrational energy of the system has changed. This is equivalent to saying that the flexibility of the system has been altered, which in terms of a protein, means that the number and/or strength of non-covalent bonds has changed which, in turn, means that atoms have been displaced. Therefore, changes in heat capacity as a function of temperature (or other variable) are an indication of conformational change.

A plot of the logarithm of affinity as a function of reciprical temperature generates a van't Hoff plot, an idealized representation of which is shown below. The slope of the line is the enthalpy change upon interaction and the y-intercept is the change in entropy. Curvature in this plot reflects variation in enthalpy change due to conformational change.

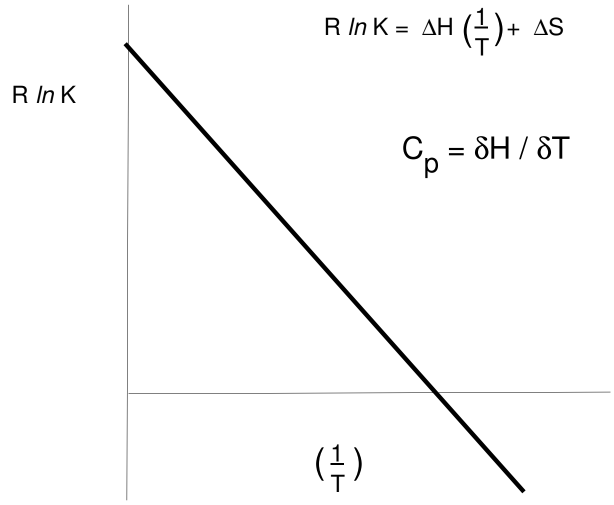

Figure 1.

Forward and reverse kinetic rate constants can also be related to energy changes involved in formation and breakage of complexes. If G_F and G_C represent the energy of the unbound and complexed system, then $\Delta G = G_C - G_F$ is the free energy change that determines the affinity of interaction (Equation 13).

Reaction rates are determined by an energy term that is independent of affinity. By analogy to standard chemical reaction kinetic formulations, If G_A represents an 'activation' energy barrier that separates free and complexed states, then the rate of complex formation is reduced by the energy difference $\Delta G_f = G_A - G_F$, and the rate of dissociation is attenuated by the energy difference $\Delta G_r = G_A - G_C$.

$$k_f = k_{df}\, e^{-(\Delta G_f/RT)}$$
$$k_r = k_{dr}\, e^{-(\Delta G_r/RT)}$$

where k_{df} and k_{dr} are the diffusion-limited rate constants that determines the rate of encounter and dis-encounter of non-interacting particles.

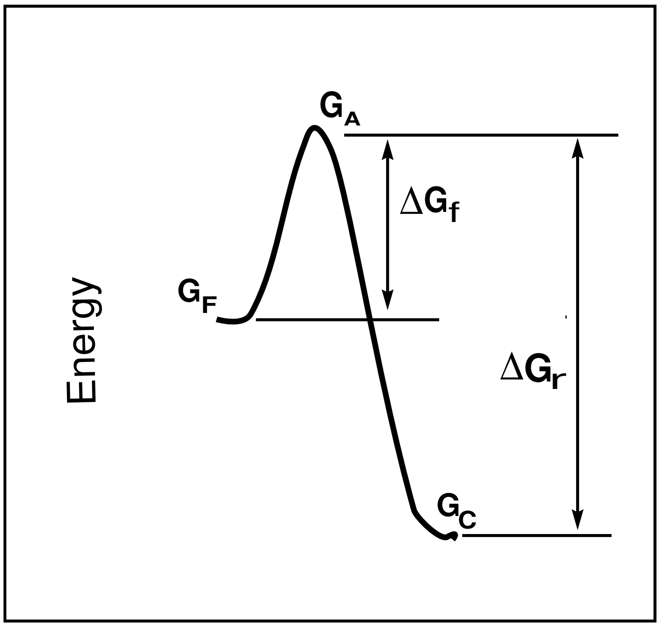

Figure 2.

G_A comprises an entropic contribution that reflects the statistically limited number of productive collisions between interacting molecules, and an enthalpic contribution from any conformational changes that are required to potentiate complex formation. As in the discussion of the relationship between free energy and affinity, one order of magnitude difference k_f or k_r results from 1.4 kcal mol^{-1} variation in ΔG_f or ΔG_r, respectively. Amino acid substitutions that affect kinetic rates can involve any combination of G_F, G_C, and G_A.

This brief discussion indicates that careful measurements of affinity of protein-protein or other macromolecular interactions can provide significant information about protein structure and stability. The free energy changes that accompany the formation of a macromolecular complex arise from the positions and separations of the various atom types that make up these molecules. These are the same considerations involved in the modeling of protein folding. Therefore, although measurements of interaction affinities has practical importance for understanding some disease processes, or selecting optimal antibodies for an immunochemical or biotechnological application, studies of this type can also address fundamental issues of macromolecular biophysics.

Simulation

The conversion of the equations that quantitatively describe the physical chemistry of molecular interactions into algorithms that emulate the process of macromolecular interactions during size-exclusion chromatography is fundamentally related to a body of work that developed simulations of the sedimentation properties of systems of interacting molecules during ultracentrifugation (e.g., Cox, 1965a,b, 1967, 1969, 1971). However, in contrast to separation of macromolecules on the basis of intrinsic mass density characteristics, the partitioning of molecular complexes by size-exclusion chromatography effectively modulates, to some extent, the reaction processes under study. The basis and implications of this phenomena, which affect all size-exclusion chromatography based methods, will be discussed later.

Basics. A primary assumption of the current algorithm is that the role of the chromatography matrix is to 'map' a characteristic transport velocity onto constituent molecules and their complexes and that this process does not modify molecular interactions. The column itself is represented as a linear array of 'cells' each of which corresponds to a subunit of column volume. For instance, a column of 1 ml volume could be represented as an array of 1000 cells of volume 1 μl or 200 cells of volume 5 μl; choice of number of cells and cell-size is determined in practice by availability of computing resources.

Prior to the initiation of a 'run,' concentrations of free and complexed constituents are established by iterative execution of the numerical representation of Equation 6. If T is the time assigned for preequilibration, and Δt is the microscopic time element chosen to be sufficiently small to keep changes in concentration small during each iteration, then the following equations are evaluated iteratively $T / \Delta t$ times.

$$\Delta c = (k_f\, ab - k_r\, c)\ \Delta t \qquad (14)$$

$$c = c + \Delta c \qquad (14a)$$

$$a = a - \Delta c \qquad (14b)$$

$$b = b - \Delta c \qquad (14d)$$

Similar expressions are used for the case of self association. Because two moles of A are consumed to form one mole of C, Equation 14b is replaced by

$$a = a - 2\,\Delta c \qquad (14e)$$

There is no expression corresponding to equation 14d. Analogous, but slightly more complex representations of bivalent interactions, competitive interactions, and oligomer formations are found in the discussion of the algorithm

Protein(s) are 'loaded' onto the column by assigning appropriate concentrations to a precolumn zone which consists of a sufficient number of cells to represent the size of the sample; *i.e.*, if each cell has been assigned a 1 μl volume, five cells correspond to an experimental sample of 5 μl. All proteins in the sample 'precolumn' migrate with unitary velocity and without dispersion. In the column array proper, each constituent and complex migrates with its assigned transport velocity. Transport of mass from cell to cell by a displacement with a gaussian distribution about a mean that corresponds to the assigned velocity. This allows for fractional velocities (which reduces the number of cells required to represent a column) and minimizes the effect of numerical dispersion on the shape of eluted bands. (Note: numerical dispersion refers to the splitting of the contents of one cell as the result of a fractional velocity; i.*e.*, if $v = 2$, then the contents of cell j are transferred to cell $j + 2$; $j + 4$; $j + 6$; ... in successive iterations of the simulation. However if $v = 2.5$, the contents of cell j are transferred to $j + 2$ **and** $j + 3$; $j + 4$**,** $j + 5$ **and** $j + 6$; $j + 5, j + 6, j + 7$, **and** $j + 8$ ... in subsequent iterations.)

The gaussian transport strategy also creates a device to represent the band spreading that occurs during chromatography due to physical dispersion that results from incomplete chromatographic partitioning, flow irregularities, edge effects, and possibly other physical effects that cause dispersal of solute observed as band broadening. The standard deviation of the gaussian distribution is used as a dispersion factor. In contrast to thermodynamic band broadening resulting from diffusion driven by a concentration gradient, stochastic or physical dispersion is concentration independent. Diffusion and dispersion parameters are oppositely related to the molecular weight of the molecule; small molecules rapidly diffuse but have small dispersion parameters; large molecules diffuse slowly but have highly dispersive chromatography properties.

The chromatography run is simulated as an alternating series of transport and relaxation steps. Transport occurs 'instantaneously;' relaxation refers to the association/dissociation reactions that occur as a consequence of the changes in constituent and complex concentrations that result during the transport step. The term 'relaxation' is chosen to reflect the anticipated general case that equilibration does not occur during the short time represented by each iteration cycle. The user selects the time represented by each iteration in a manner that is consistent with the number of cells selected to represent the column, the number of run cycles, and relative constituent velocities

Consider a simulation that requires component A to elute at 20 minutes of a 30 minute run.[2] If the column length has been assigned as 1000 cells, and the time for each cycle is 1 second, then the velocity of component A is 0.83 cells/cycle. It is generally preferable to have velocities greater than one, to avoid significant 'back flow' that can result from the gaussian formulation for transport. In this example, this can be accomplished by either representing the column as 2000 cells, or increasing the absolute time per cycle.

Following transport through the column, the simulated molecule enters a post-column zone or 'monitor queue' in which all components pass with unitary velocity. In addition to representing the tubing between a chromatography column and detector in an experimental system, the monitor queue provides a convenient means to sum or integrate the material that emerges from the column, which when compared to the quantities at the start of the run, can be used to check for potential numerical artifacts.

Algorithm. SCIMMS is organized as two blocks of subroutine calls. The first series of subroutines is executed once at the begining of each simulated run and is used to set up the parameters for each run. The second block of subroutines is executed iteratively during the simulated run; each iteration represents one cycle of relaxation and transport.

```
c-----------------------------------------------------------------------------
c     Set Up:
c       load Gaussian distribution table          (GAUSS)
c       input column parameters                   (COLUMN)
c       input protein input file list             (PRO_FILE)
c       input protein parameters                  (PROTEINS)
c       calculate weighted extinctions            (EXTINCTION)
c       create unique output file index           (FILE_NUM)
c       saturate column if chosen                 (SATURAT)
c       apply sample to column                    (LOADER)
c       pre-run equilibration                     (ITER_KIN)
c       setup full output                         (TERM_WRITE)
c       setup plot output                         (PLOT_WRITE)
c       document run                              (LOG_DAT)
c---------------------------------------------------------------------------
```

GAUSS: Reads into an array the first half of a normal distribution table (0.0 –> 0.5) and creates the remainder. These values are used to control the transport algorithm.

COLUMN: Opens and reads the file **column_inpt.dat.** an example of which is shown:

```
200     !column length (cells)
0.0     !column volume (ml)
010      !monitor queu length (cells)
4       !sample size (cells)
150     !run length (cycles)
200      !pre-run length (cycles)
0.02     !time increment (seconds)
```

[2] This value for run time need not equal the experimental run time but can refer to the portion of an experimental chromatogram that is of quantitative interest.

```
0.05     !max change in concentration (fraction)
2.0      !time per cycle (seconds)
1        !number of diffusion iterations per cycle
6        !gaussian spread
0.0      !flow rate (ml/min)
2        !saturate with B2 (1 = yes; 2 = no)
```

The text following the exclamation point is ignored by the program and identifies the parameter. Most of the parameters are self-explanatory and are used to establish the physical characteristics of the simulated column. The **gaussian spread** provides the number of cells to each side of the mean cell for which possible transport of material is calculated. The **saturate** parameter allows for a pre-equilibration of the column with component B2 at its initial concentration; and maintains that concentration throughout the run.

Two paramaters are not involved in calculations during the simulation. The ***column*** **volume** and ***flo rate*** parameters are optional. If both are zero, then the default output of the simulation documents the elution profile as a function of time. If the **flo rate** term is finite while the **column volume** term remains zero, then the output provides the elution profile as a function of volume. If both **flo rate** and **column volume** are finite, then the elution volume is generated as a function of Ve/Vt, elution volume related to total column volume. (A finite **column volume** coupled with a nil **flo rat***e* is not meaningful; output reverts to the default status as a function of time in minutes.)

PRO_FILE: Opens and reads the file **proteins_inpt.lst**, an example of which is shown:

```
proteins_in004.dat
proteins_in005.dat
proteins_in006.dat
proteins_in007.dat
proteins_in008.dat

proteins_in001.dat
proteins_in002.dat
proteins_in003.dat
```

The entries in this file are the names of setup files that will be subsequently read by the next subroutine (**PROTEINS**). The names of these files are arbitrary. Each setup will be executed in turn; a single set of column parameters (as provided by column_inpt.dat) will be used for the entire series of runs. The blank line between proteins_in008.dat and proteins_in001.dat will cause the simulation series to be interrupted at that point, The file proteins_inpt.lst can be maintained as a 'master file' which can be edited in blocks for various simulation purposes.

PROTEINS: Opens and reads (one per run) the protein parameter setup files obtained by **PRO_FILE**. An example of a protein parameter file is shown:

```
01.000  050000.  001.500  01.000  00.250  00.600  !con mw vel extcf dif disp (pr A)
00.000  050000.  001.500  01.000  00.250  00.700                  !  (protein B1)
00.000  025000.  001.000  01.000  00.250  00.400                  !  (protein B2)
1.8    0.25   0.4                                        !vel(0)   dif(0)   disp(0)
02.10  01.75  02.10  02.30  02.40                              !velocities(4 -->  8)
02.45  02.50  02.50  02.50  02.50                              !velocities(9 --> 13)
0.60  0.65  0.80  0.90  0.90                                   !dispersion(4 -->  8)
0.90  0.90  0.90  0.90  0.90                                   !dispersion(9 --> 13)
0.25  0.25  0.50  0.50  0.50                                   !diff_coefs(4 -->  8)
0.50  0.50  0.50  0.50  0.50                                   !diff_coefs(9 --> 13)
0.10e+06                                                           !kf A:A    kf(0)
0.10e-01                                                           !kr A:A    kr(0)
0.00e+04                                                           !kf A:B1   kf(1)
0.00e-01                                                           !kr A:B1   kr(1)
0.00e+05                                                           !kf A:B2   kf(2)
0.10e-00                                                           !kr A:B2   kr(2)
```

```
0.10e+07                                    !kf C:C    kf(3)   C = A:A
0.10e-00                                          !kr C:C    kr(3)
1                                             !valence of A for B1

! concentration in mg/ml
! mw in daltons
! migration velocity in cells per cycle
! extinction coefficient as effective absorbance units per mg/ml
! diffusion coefficient as percent equilibration per cycle
! dispersion coefficient as gaussian spread per translation
!
```

The first three lines define the properties of the three molecular species (A, B1, and B2; identified within the algorithm as species 1,2, and 3, respectively) which are manipulated in during the simulation. Each species provides specific functional features that can be manipulated to establish various chromatographic strategies.

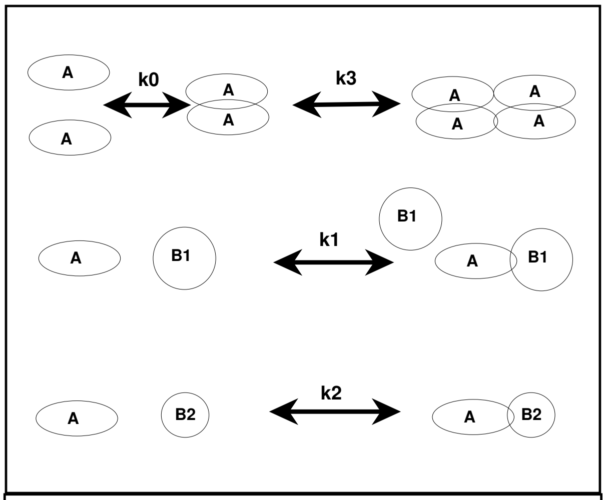

Schematic representation of molecular identities and rate constants used in SCIMMS. Species A is capable of self-association governed by forward and reverse rate constants k0; dimers may further aggregate as determined by rate constants k3. Species A is capable of mono- or bivalent interactions with B1 (rate constants k1). Species B2 interacts monovalently with A competing for the site of B1 interaction (rate constants k2).

Figure 3.

The parameters contained in these lines are concentration (mg/ml), molecular weight (daltons), velocity (cells/cycles), extinction coefficient (in relative units to mg/ml[3], diffusion parameter (fractional diffusion equilibrium achieved in each cycle, and dispersion coefficient (standard deviation of gaussian distribution) . The fourth line contains the velocity, diffusion, and dispersion parameters that characterize species 0, which can represent either a dimer of component A or a bivalent complex of component A and two molecules of component B1.

Lines five through ten contain the velocity (5,6) , dispersion (7,8), and diffusion (9,10) parameters of species 4 through thirteen. Species 4 is the monovalent complex formed by component A and B1. Species 5 is the monovalent complex formed by A and B2. Species 6 through 7 are higher order aggregates of A; species n contains n–4 dimers of A.

Lines 11 and 12 contain the forward and reverse kinetic rate constants that govern dimerization of A.

Lines 13 and 14 contain the forward and reverse kinetic rate constants that determine interaction between A and B1; in the case of bivalent interaction between A and B1, it is assumed that both binding sites are identical.

Lines 15 and 16 contain the forward and reverse rate constants that control interactions between A and B2. Bivalent interactions between A and B2 are not allowed.

Line 17 contains the valence of A for B1; the default value is one. The valence must be one for

[3] If the extinction coefficient is unitary, output is effectively in units of concentration.

competition simulations involving B1 and B2.

EXTINCTION: Computes the molecular weights and extinction coefficients for the complexes formed by A, B1, and B2.

FILE_NUM: Opens and reads the file **ksym_rec.dat**. This file contains a single four digit integer. This number is read, incremented by one unit, and rewritten to the file. The number that was originally read becomes the suffix for the files generated by the simulation, providing a mechanism for systematically 'unique' file names.

SATURAT: If the saturation parameter has been set to choose saturation, then a prerun iteration is used to introduce component B2 at the origin of the column and to transport B2 through the column; this process is repeated sufficient times to equilibrate the column[4].

LOADER: The total column length is the sum of sample size (SS) and transport column length (CL). This subroutine places calculated molar concentrations of A, B1, and B2 in the first SS cells.

ITER_KIN: Numerically computes the formation of molecular complexes by iterative evaluation of appropriate kinetic expressions. Prior to initiation of kinetic iteractions, the concentration change is calculated and compared to the fractional change permited by the parameter **delta_max**. If necessary, a new value of **t_inc** is calculated and used through the remeainder of the simulation. This new value is noted in the out and is recorded in the log file.

Several cases are specifically configured.

Dimerization:

$$\Delta c = (k_f\, a^2 - k_r\, c)\ \Delta t$$
$$c' = c + \Delta c$$
$$a' = a - 2\Delta c$$

Heterologous Monovalent:

$$\Delta c = (k_f\, ab - k_r\, c)\ \Delta t$$
$$c' = c + \Delta c$$
$$a' = a - \Delta c$$
$$b' = b - \Delta c$$

Heterologous Bivalent:

$$\Delta c = (k_f\, ab - k_r\, c)\ \Delta t$$
$$c' = c + \Delta c$$
$$a' = a - \Delta c$$
$$b' = b - \Delta c$$

(d represents a B-A-B complex)

$$\Delta d = (k_f\, cb - k_r\, d)\ \Delta t$$
$$d = d + \Delta d$$
$$c' = c - \Delta c$$
$$b' = b - \Delta c$$

---

[4]During the course of the run, B2 continues to be introduced to the column by subroutine MIGRATE

Competitive:

$$\Delta c_1 = (k_f\, ab_1 - k_r\, c_1)\ \Delta t$$
$$c_1' = c_1 + \Delta c$$
$$a' = a - \Delta c$$
$$b_1' = b_1 - \Delta c$$
$$\Delta c_2 = (k_f\, ab_2 - k_r\, c_2)\ \Delta t$$
$$c_2' = c_2 + \Delta c$$
$$a' = a - \Delta c$$
$$b_2' = b_2 - \Delta c$$

Oligomerization:

d_n represents an oligomer of n A-A dimers. For simplicity, it is assumed that each d_n arises from the association of a free d_1 with a molecule of d_{n-1}

$$\Delta d_2 = (k_f\, d_1 d_1 - k_r\, d_2)\ \Delta t$$
$$d_2' = d_2 + \Delta d_2$$
$$d_1' = d_1 - 2\,\Delta d_2$$

Note that d_n, has n-1 sites for dissociation; thus the molarity of dissociation sites must be incorporated.

$$\Delta d_3 = (k_f\, d_2 d_1 - 2\, k_r\, d_3)\ \Delta t$$
$$d_3' = d_3 + \Delta d_3$$
$$d_1' = d_1 - \Delta d_2$$
$$d_2' = d_2 - \Delta d_3$$

For n > 3 , dissociation at different sites will generate breakdown products of diverse sizes; therefore there is no longer an equimolar ratio of moles of oligomer broken and moles of suboligos formed. In general, n-2 moles of dn are required to form 2 moles of all possible sub-oligos. It is assumed that dissociation at all sites is equally likely. In the following, d_{n+} and d_{n-} represent oligo n formed or broken respectively.

$$\Delta d_{4+} = k_f\, d_3 d_1 \Delta t$$
$$\Delta d_{4-} = 2\, k_r\, d_4\ \Delta t$$
$$d_4' = d_4 + \Delta d_{4+} - \Delta d_{4-}$$
$$d_1' = d_1 - \Delta d_{4+} + 2\,\Delta d_4/3$$
$$d_2' = d_2 + 2\,\Delta d_4/3$$
$$d_3' = d_3 - \Delta d_{4+} + 2\,\Delta d_4/3$$

Similar series of equations for higher order magnitude. We have arbitrarily chosen a maxim n of 9 on the assumption that experimental conditions that generate n > 9 will not provide useful experimental data.

When operated in the pre-equilibration mode, the subroutine returns the final values of the various constituents and aggregates. These numbers are compared to the values obtained at the penultimate cycle to confirm convergence, and, where possible, to explicitly calculated values to confirm accuracy.

TERM_WRITE: Called twice. Reports setup parameters to terminal and to file **ksm_(#).chr**, where (#) represents unique identification number.

PLOT_WRITE: Opens file **ksm_(#).out** which will contain the x and y values generated by the simulation; opens file **ksm_(#).mat** which contains only the y values.

LOG_DAT: Reads the file **scm10_log.dat** which contains all the protein and column input parameters. The value recorded for the parameter will either be the set-up value or the value calculated by **ITER_KIN** to satisfy the **delta_max** parameter. The file **scm10_log.da**t is an ASCII file which can be edited. The first line reports the number of data lists in the file. This value is used to control the formatted reading of the remainder of the file. As set by the parameter **lists** in the **LOG_DAT** subroutine, each page of the chronicle file contains four lists of data. This value may be changed by editing the subroutine and recompiling the program. The chronicle file can contain up to 200 lists, as controlled by the parameter **max_records** in the subroutine. This value may also be changed by editing the subroutine and recompilation.

Because **scm10_log.dat** is of restricted size, it is recommended that the chronicle file be systematically copied. The replicated file should be renamed to serve as an archival record if warrented. The working file is then edited to reduce its size. The easiest way to accomplish this is to simply change the value for the number of lists to 0 in the first line. This causes the subrouine to read none of the existing data, and to write only the current indput data values.

Example scm10_log.dat file:

2

Date:	30-AUG-93	30-AUG-93
Time:	11:11:30	12:22:00
Infile:	proteins_in001	proteins_in003
Outfile:	ksm_4055.chr	ksm_4056.chr
A conc:	1.000000	1.000000
A mw:	25000.	25000.
A veloc:	1.500000	1.500000
A extcf:	1.000000	1.000000
A dif:	0.250000	0.250000
A disp:	0.500000	0.500000
ValenceA:	1	1
B1 conc:	0.000000	0.000000
B1 mw:	50000.	50000.
B1 veloc:	1.500000	1.500000
B1 extcf:	1.000000	1.000000
B1 dif:	0.250000	0.250000
B1 disp:	0.700000	0.700000
B2 conc:	0.000000	0.000000
B2 mw:	50000.	50000.
B2 veloc:	1.800000	1.800000
B2 extcf:	1.000000	1.000000
B2 dif:	0.250000	0.250000
B2 disp:	0.700000	0.700000
Saturate:	No	No
AA veloc:	1.800000	1.800000
AA dif:	0.250000	0.250000
AA disp:	0.700000	0.700000
AB1 velc:	1.800000	1.800000
AB1 dif:	0.250000	0.250000
AB1 disp:	0.600000	0.600000
AB2 velc:	1.800000	1.800000
AB2 dif:	0.250000	0.250000
AB2 disp:	0.650000	0.650000
ABB velc:	0.000000	0.000000
ABB dif:	0.000000	0.000000
ABB disp:	0.000000	0.000000
C2 veloc:	0.000000	0.000000
C2 dif:	0.000000	0.000000
C2 disp:	0.000000	0.000000
C3 veloc:	0.000000	0.000000
C3 dif:	0.000000	0.000000
C3 disp:	0.000000	0.000000
C4 veloc:	0.000000	0.000000
C4 dif:	0.000000	0.000000
C4 disp:	0.000000	0.000000
C5 veloc:	0.000000	0.000000
C5 dif:	0.000000	0.000000
C5 disp:	0.000000	0.000000
C6 veloc:	0.000000	0.000000
C6 dif:	0.000000	0.000000
C6 disp:	0.000000	0.000000
C7 veloc:	0.000000	0.000000

C7 dif:	0.000000	0.000000
C7 disp:	0.000000	0.000000
kf_AA:	0.00E+00	0.10E+05
kr_AA:	0.10E+00	0.10E+00
kf_AB1:	0.00E+00	0.00E+00
kr_AB1:	0.00E+00	0.00E+00
kf_AB2:	0.00E+00	0.00E+00
kr_AB2:	0.00E+00	0.00E+00
kf_CC:	0.00E+00	0.00E+00
kr_CC:	0.00E+00	0.00E+00

(Continues on next page)

Col_len:	500	500
SampS z:	100	100
MonQ:	10	10
Run_len:	500	500
PreEquil:	200	200
Time_cyc:	1.800000	1.800000
Time_inc:	0.020000	0.020000
MaxDelta:	0.050000	0.050000
GausSprd:	6	6
Dif_cycs:	1	1
ColVl(ml):	0.000000	0.000000
FloRate:	0.000000	0.000000

```
c--------------------------------------------------------------------
c     Column Run:
c       calculate compositions            (ITER_KIN)
c       advance proteins                   (MIGRATE)
c       passage monitor queue              (MONITOR)
c       calculate terminus
c           absorbance                  (ABSORBANCE)
c       output elution status               (REPORT)
c       diffusion cycles               (DIFFUSION_1)
c       output sums; close files              (SUMS)
c-------------------------------------------------------------
```

The **Column Run** set of subroutines (with the exception of **SUMS**) are iteratively repeated for the number of cycles specified by *run length* in column_inpt.dat. **SUMS** is called once at the completion of the run cycle.

ITER_KIN: This subroutine is the only subroutine used by both the set-up and execution components of the simulation. See above for discussion.

MIGRATE: Controls transport of constituents and aggregates through the simulated column. The assigned velocity in cells/cycle is used as the mean of the gaussian distribution and the dispersion coefficient is the corresponding standard deviation. The routine calculates the quantity of material transferred to the cell that contains the mean position, as well as preceding and following cells as defined by the parameter, ***sprd***.

For a detailed description of the methods to numerically implementing the gaussian transport, please see Stevens, 1986

MONITOR: Advances components through the monitor queue one cell each cycle.

ABSORBANCE: Calculates the total

absorbance of the components found in the terminal cell of the monitor queue based on individual constituent concentrations and extinction coefficients.

REPORT: Writes to terminal and output files the ‘absorbance’ at the monitor terminus. Not all cycles are reported for long runs.

DIFFUSION: Emulates thermodynamic (concentration gradient – driven) band spreading. Rather than use an absolute diffusion coefficient, the routine obtains the difference in concentrations in adjacent cells. If each cycle was sufficiently long, complete diffusion equilibrium would result in equal concentrations in adjacent cells. The diffusion parameter specifies the degree to which diffusion equilibrium is reached.

Examples.

The following examples were generated with a simulated column having the following arbitrary parameters:

500 !column length (cells)
0.0 !column volume (ml)
010 !monitor queu length (cells)
4 !sample size (cells)
500 !run length (cycles)
200 !pre-run length (cycles)
0.02 !time increment (seconds)
0.05 !max change in concentration (fraction)
1.8 !time per cycle (seconds)
1 !number of diffusion iterations per cycle
6 !gaussian spread
0.0 !flow rate (ml/min)
2 !saturate with B2 (1 = yes; 2 = no)

Standard Curve. The velocity of a monomeric protein of MW 25000 was arbitrarily assigned as 1.5 cells/cycle and that of a dimer of molecular weight 50000 as 1.8 cells/cycle. These selections generate the following standard curve assuming an idealized relationship between the elution time and the logarithm of the molecular weight.

Calibration: MW vs Elution Position

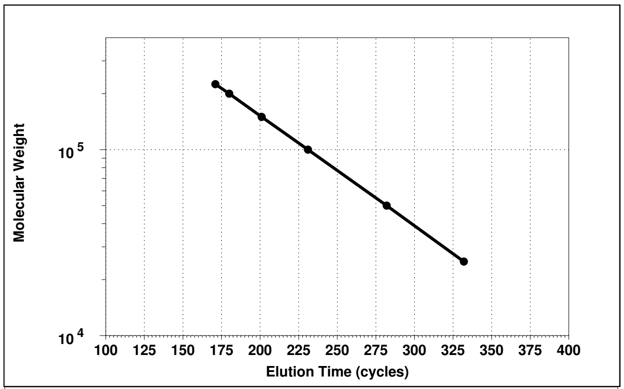

Relationship between elution position and molecular weight of molecules on a simulated column of 1000 cells. The monomer and dimers are assumed to have velocities of 1.5 and 1.8 cells/cycle; this defines the positions of aggregates containing two, three, four, five or more dimers. Assuming an excluded volume of one third the column volume, the maximum velocity is 3 cells/cycle.

Figure 4.

Two molecular species with assigned velocities of 1.5 and 1.8 cells/cycle are resolved as shown:

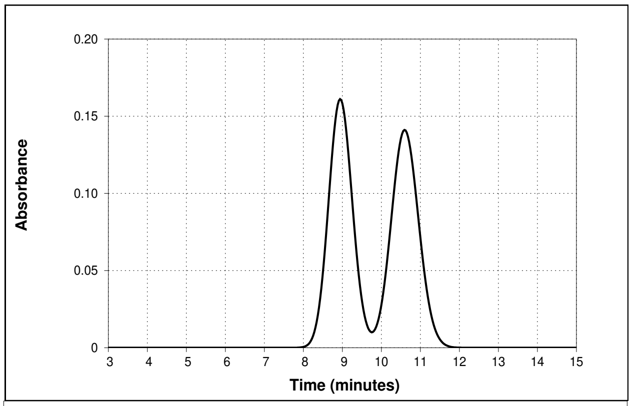

Elution profiles for simulated molecules corresponding to monomer of molecular weight 25,000 and a dimer of molecular weight 50,000 with assigned velocities of 1.5 and 1.8 cells/cycle respectively. Column consisted of 500 cells with a run length of 500 cycles representing 1.8 second each. Sample of 4 cells contained 1 mg/ml of each species.

Figure 5.

The dispersion parameter was set at 0.5 for monomer and 0.7 for dimer; both diffusion parameters were 0.25.

Modes of simulated chromatography.

Depending upon the values selected for the four potential pairs of kinetic rate constants incorporated in the simulation, various experimental strategies can be emulated.

	k_0	k_1	k_2	k_3
Homologous	+	0	0	0
Heterologous	0	+	0	0
Competitive	0	+	+	0
Oligomeric	+	0	0	+
Inhibitive	+	0	+	0

Homologous Association. Homologous or self association has been studied in our laboratory as dimerization of human antibody light chains (Stevens et al., 1980; Stevens & Schiffer, 1981) and dimerization of various phospholipases (Myatt et al., 1991).

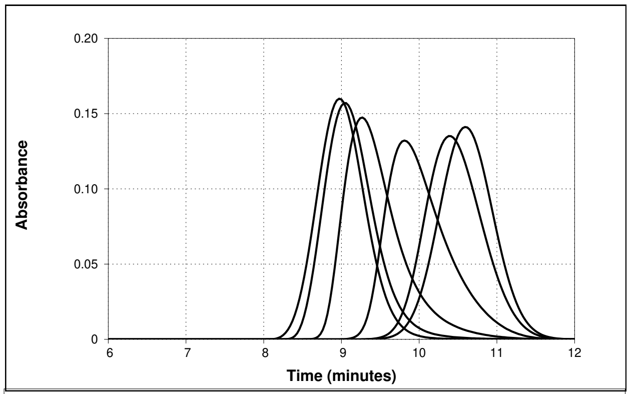

Simulated dimerization (homologous association). Affinity of self-association is inversely related to time required for elution. Dimer formation for varied affinity was determined by a fixed k_r of 0.1 s^{-1}. From left to right, peaks represent dimerization affinities of 10^8, 10^7, 10^6, 10^5, 10^4 and 0 M^{-1}. The asymmetry most notable in the peaks generated for affinities of 10^5 and 10^4 M^{-1} is characteristic of dynamic interactions during size-exclusion chromatography.

Figure 6.

In SCIMMS, species A is the only constituent capable of homologous interactions. These interactions are governed by the forward and reverse rate constants kf(0) and kr(0). Dimerization of A (protein 1 in the algorithm) creates a constituent identified as protein 0 whose velocity, diffusion coefficient, and dispersion coefficient are identified as vel(0), dif(0), and disp(0), respectively. The extinction coefficient of an A–A dimer is equal to that assigned to A.

Heterologous Association (Monovalent)
Association of two different macromolecular species is typified by antibody–antigen interactions or protein–nucleic acid interactions. An intact IgG which exhibits two antigen combining sites provides bivalent interaction; an antigen binding fragment (Fab) formed by enzymatic digestion of an immunoglobulin or by expression in recombinant bacteria is a monovalent receptor.

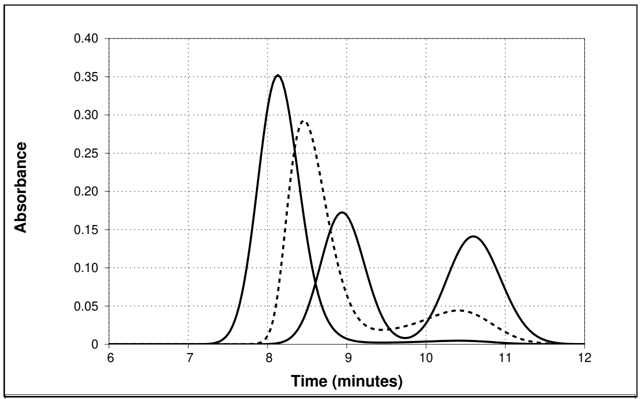

Simulated heterologous association. The smaller species is assigned a molecular weight of 25000, a concentration of 1.0 mg/ml, a velocity of 1.5, and an extinction coefficient of 1.0; the larger species is assigned a molecular weight of 50000, a concentration of 2.0 mg/ml, a velocity of 1.8, and an extinction coefficient of 0.5. The complex formed by one molecule of each species is assigned a velocity of 2.0 cells/cycle. Affinities from left to right are 10^8, 10^6, and 0 M^{-1}; for both non-zero affinities, k_f was fixed as 10^5 M^{-1} s^{-1}.

Figure 7.

In SCIMMS, species A can bind one or two molecules of species B1 (protein 2), as set by the valence value assigned in the protein parameter file. Interactions between A and B1 are determined by rate constants kf(1) and kr(1). The A–B1 complex is identified as protein 4 with correspondingly indexed velocity, diffusion, dispersion and extinction coefficient.

Heterologous Association (Bivalent)
Bivalent interactions include, as noted above, the binding of antigen by intact IgG. An antigen that exposes two identical epitopes to Fabs, such as was found in a study of rheumatoid factor binding to immunoglobulin (Stevens, 1986) is another example. The case of an antigen having two non-identical epitopes

capable of simultaneous binding by two different antibodies is not currently covered.

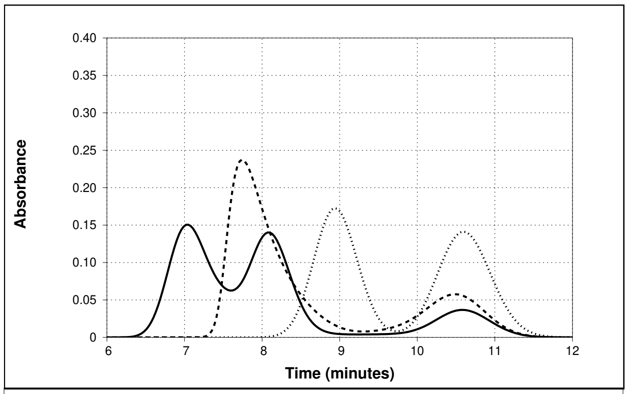

Simulated elution profiles of heterologous interactions in which one of the components is bivalent. The molecular weight, concentration, velocity, and extinction parameters are as reported in the previous illustration of monovalent heterologous association. The velocity of species 0 (the B1-A-B1) complex is 2.35 cells/cycle. Note that because species A is bivalent, excess binding sites relative to the concentration of B are present. Therefore, a fraction of A is unbound and elutes at the free position (at approximately min 10.6).

Figure 9.

Competitive Association. Size-exclusion chromatography provides a convenient way to demonstrate that two monoclonal antibodies bind to the same or overlapping epitopes. Alternatively, an intact antibody and the Fab formed by its enzymatic digestion necessarily bind to the same epitope with, nominally, the same thermodynamic and kinetic properties. Because these two molecules are of different size, exchange of intact antibody and Fab in complexes with antigen alter chromatography behavior in a manner that is a potentially useful means of extracting kinetic rate constants.

In SCIMMS, species A can bind either B1 or B2, but not both simultaneously. Therefore, when both sets of rate constants, [kf(1), kr(1)] and [lf(2), kr(2)], are non-zero, competition between B1 and B2 takes place. If either the k(1) rate constants differ from the k(2) rate constants, or B1 and B2 transport through the column at different rates, then the presence of competition will be reflected in alterations of the elution profile.

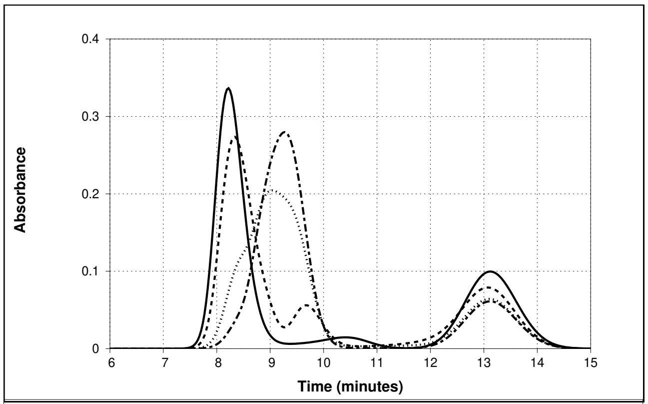

Simulated competition between species B1 and B2 for binding to A. Parameters defining species A and B1 are as in the previous illustration of heterologous monovalent interaction; affinity is 10^7 M^{-1} (kf = 10^5 M^{-1} s^{-2}, kr = .01 s^{-1}). Species B2 has an assigned concentration of 1 mg/ml, molecular weight of 10000, extinction coefficient of 1.0, diffusion parameter of 0.4, dispersion parameter of 0.3, and a velocity of 1.3 cells/cycle. The affinities of A–B2 interaction are 0 (——), 10^7 (- - - -), 10^8 (·······), and 10^9 (-·-·-) M^{-1}; for non-zero affinities kf(2) = 10^5 $M^{-1}s^{-1}$.

Figure 10.

One potential application for the competition mode of simulation is to evaluate the ability of peptides or other small molecules to act as antagonists for interaction between other molecules; *i.e.*, for drug design studies. In many of these studies, the affinity of the smaller molecule may be weak, and because of the differences in size between the small antagonist and the larger interacting macromolecule, be quickly separated by the chromatography process. These factors will reduce competition and obscure the resulting chromatography signal. By saturating the chromatography column with the competitor, the experimenter assures that the interacting macromolecules are always in the presence of a known concentration of antagonist, and maximize the signal resulting from competition. This capability is obtained in the simulation by setting the **saturate** parameter in the **column_inpt.dat** file and is illustrated below.

Oligomeric Association. The formation of high-order multi-subunit oligomers is found in several protein-based disease process, including fibril formation by sickle cell hemoglobin and amyloid formation by a number of proteins, including antibody light chains.

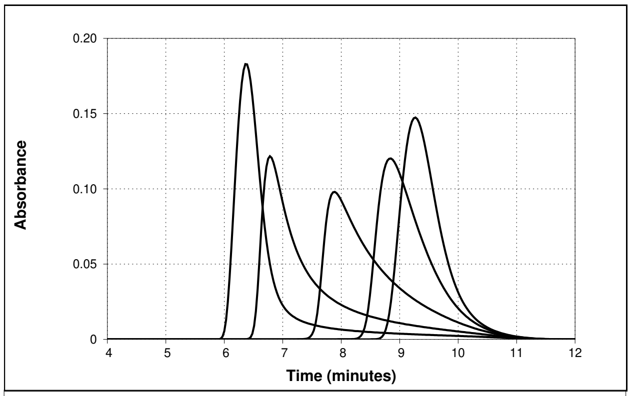

Simulated oligomerization following dimer formation. Increasingly early elution reflects increasing affinity of oligomer creation. In each case, dimerization occurs with k_f and k_r of 1.0 x 10^5 $M^{-1}s^{-1}$ and 0.1 s^{-1}, respectively. Oligomer formation for varied affinity was determined by a fixed k_r of 0.1 s^{-1} and, from left to right, k_f values of 1 x 10^7, 10^6, 10^5, and 10^4 $M^{-1}s^{-1}$, respectively.

Figure 11A.

```
01.000  025000.  001.500  01.000  00.250  00.500  !con mw vel extcf dif disp (protein
00.000  050000.  001.500  01.000  00.250  00.700           !!  (protein B1)
00.000  050000.  001.800  01.000  00.250  00.700           !  (protein B2)
1.8     0.25   0.7                                  !vel(0)   dif(0)   disp(0)
01.80  01.80  02.22  02.55  02.87                   !velocities(4 -->  8)
03.00  03.00  03.00  03.00  03.00                   !velocities(9 --> 13)
0.60  0.65  0.80  0.90  0.90                        !dispersion(4 -->  8)
0.90  0.90  0.90  0.90  0.90                        !dispersion(9 --> 13)
0.25  0.25  0.25  0.25  0.25                        !diff_coefs(4 -->  8)
0.25  0.25  0.25  0.25  0.25                        !diff_coefs(9 --> 13)
0.10e+06                                            !kf A:A    kf(0)
0.10e+00                                            !kr A:A    kr(0)
0.00e+04                                            !kf A:B1   kf(1)
0.10e-01                                            !kr A:B1   kr(1)
0.00e+05                                            !kf A:B2   kf(2)
0.10e-00                                            !kr A:B2   kr(2)
0.10e+05                                            !kf C:C    kf(3)   C = A:A
0.10e-00                                            !kr C:C    kr(3)
1                                                   !valence of A for B1
```

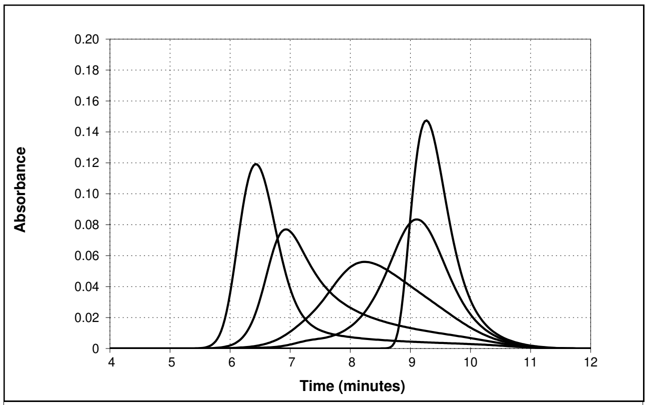

Simulated oligomerization; dimerization and oligomerization constants have the same values as in the previous illustration. Differences in the observed elution profiles result from the fact that both oligomerization rate constants are one order of magnitude smaller than in the above figure.

Figure 11B.

In SCIMMS, oligomerization occurs by setting non-zero values for [kf(0), kr(0)] and [kf(3), kr(3)]. In this model, higher order aggregation is dependent upon prior formation of dimers.[5]

Inhibitive Association. One of the goals of studying protein oligomerization that leads to clinical pathologiies is to identifiy drugs that can be used to treat the resulting conditions.

Inhibition of oligomer formation can be accomplished in the current version of SCIMMS by setting the rate constants for either B1 or B2 to non-zero values. Formation of A–B1 or A–B2 complexes reduces the concentration of A, resulting in decreased formation of A–A, thus inhibiting oligomer formation.

A future version of SCIMMS will incorporate inhibition of oligomerization at the dimer–dimer level of interaction.

Kinetic Contributions. The influence of the

[5]Note that the dimerization criteria can be effectively by-passed by setting kf(0)/kr(0) at a sufficiently high level to assure complete and stable dimer formation.

kinetics of interaction on observed chromatographic behavior can be considered in three catagories. **(1)** Equilibrated — very fast association and dissociation rates such that at each point in the solute zone, the proportions of free and associated constituents satisfy the mass action relationsihip given by Equation (1). **(2)** Static -- extemely slow dissociation rate, such that essentially no dissociation of complexes takes place during the chromatography run. In this case, discrete peaks observed in the chromatograms can be interpreted as quantitatively representing the relative concentrations of complexed and free components prior to initiation of the run. **(3)** Kinetically controlled -- Dissociation and reassociation occur during the course of the chromatography run, but at rates such that the proportion of complex at any point in the solute zone is not predicted by Equation (1).

Illustrations of each case are shown below.

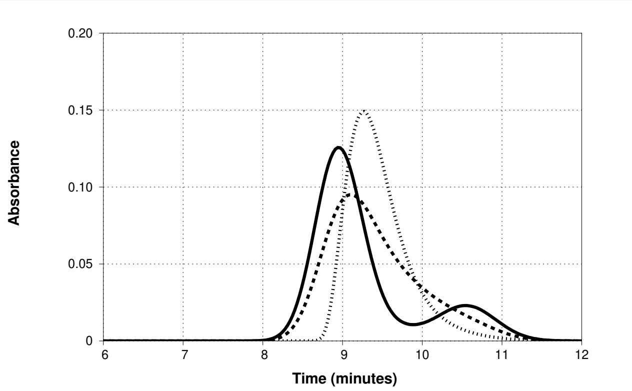

Simulated chromatograms to illustrate the contribution of kinetic rate constants in observed elution profiles. Chromatograms illustrate self-association of a 1 mg/ml sample, molecular weight 25000, monomer velocity of 1.5 cells/cycle, dimer velocity of 1.8 cells/cycle; affinity of 10^6 M^{-1} in all cases. Shapes of elution profiles reflect differences in rate constants; rapid equilibration (······), $k_f = 10^6$ M^{-1} s^{-1}; kinetically controlled elution (- - -), $k_f = 2 \times 10^3$ M^{-1} s^{-1}, static elution (——), $k_f = 2 \times 10^{-2}$ M^{-1} s^{-1}.

Figure 13.

One order of magnitude shift in the rate constants is sufficient to convert the elution profile from kinetic control to static. Note also the influence of the kinetics of oligomerization on the shape of the elution profile as can be compared in Figures 11A and 11B.

Large Zone Chromatography. When the sample size is a large fraction of the volume of the chromatography column (on the order of 20% or more), a plateau of solute is generated in which a constant concentration equal to that of the initial sample concentration is maintained. Because this condition provides for a simplified mathematical relationship between the ratio of free and associated constituents, large-zone chromatography has been an accepted method for quantitative analysis of protein–protein interactions. Large zone chromatography methods can consume significant quantities of sample, a potential disadvantage when studying expensive solutes or unique materials of limited supply, such as Bence Jones proteins obtained clinically from patients.

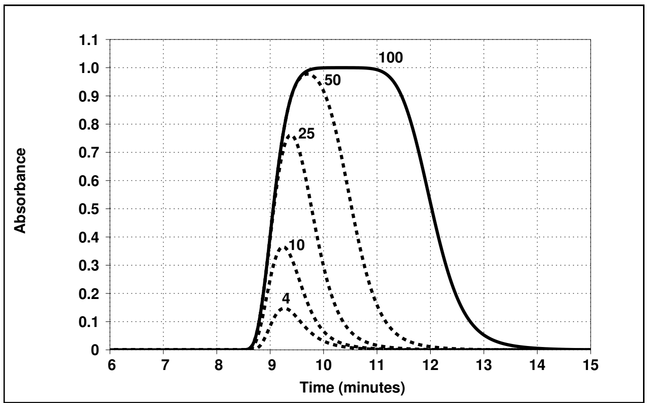

Formation of a concentration plateau with increasing sample size. Column volume was 500 cells; transition from small– to large–zone characteristics takes place between 10 to 20% of column volume in this example depicting self-association; $k_f = 10^6$ M^{-1} s^{-1}, $k_r = 0.1$ s^{-1}, MW = 25000, conc = 1 mg/ml, $vel_{mono} = 1.5$ cells/cycle, $vel_{dimer} = 1.8$ cells/cycle.

Figure 14.

In SCIMMS, large zone chromatography is accomplished simply by setting a sufficiently large value of sample size in the **column_inpt.dat file**. Although it is not a primary purpose to simulate large-zone chromatography, such simulations of an analytical strategy with quantitatively

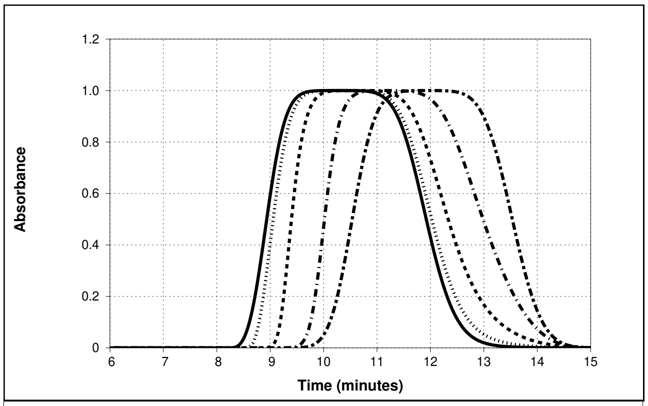

Simulated large zone chromatography of self-associating molecules. Sample size is 100 cells; other parameters are set at the values used to generate the small-zone chromatograms shown in Figure 6.

Figure 15.

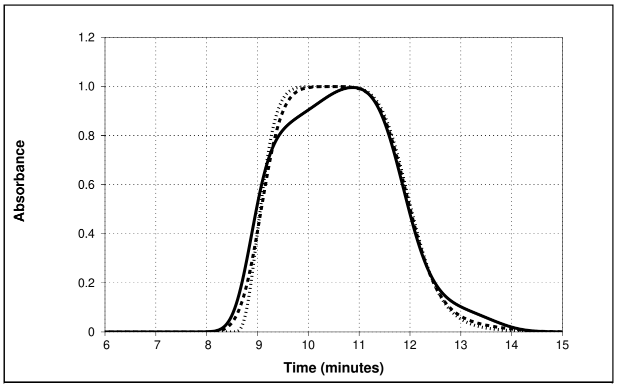

Simulated large-zone chromatograms corresponding to self-association of molecules having equivalent affinities but different kinetic characteristics. Parameter values are those that generated Figure 13; sample size is 100 cells.

Figure 16.

predictable results provides a means for evaluating the self-consistency of these algorithms.

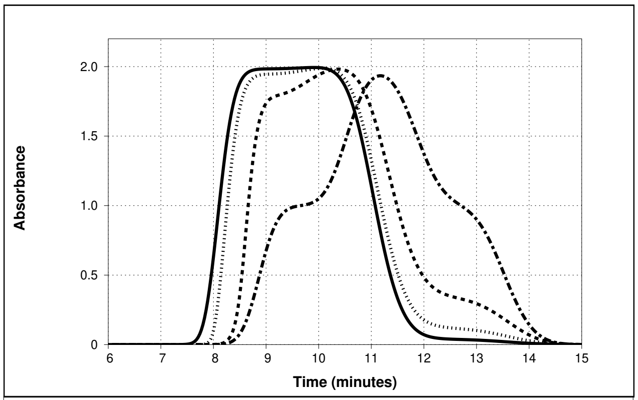

Simulated large zone chromatography of heterologous species. From left to right, affinities are 10^7, 10^6, 10^5, and 0 M^{-1}; $k_f = 10^5$ M^{-1} s^{-1} in all cases. The appearance of three lobes (or one peak with leading and trailing shoulders) in the case of K = 0 M^{-1} results from the overlap of two large zones of non-interacting species that elute with different constituent velocities.

Figure 17.

Saturation Chromatography. Saturation of the chromatography column is accomplished when one of the constituents of the interaction is present in the elution buffer; *i.e.*, a constant concentration of the constituent is present and maintained throughout the column. As with large zone chromatography, this strategy provides for simplified representation of the interaction (Hummel & Dryer, Siegel & Schumaker, 1983; Frankel et al, 1985).

As noted above for large-zone chromatography, simulation of these techniques provides a means for testing the self-consistency of SCIMMS algorithms. An example of a Hummel & Dryer type experiment is shown below.

Application of Simulation.

By optimizing rate constants that predictively emulate interactive size-exclusion chromatograms as a function of constituent concentrations, SCIMMS may be used to quantitatively analyze the kinetics and affinity of macromolecular interactions.

Step 1: For heterologous associations, fit elution profiles obtained for constituents chromatographed individually. This involves systematically varying velocity, extinction, diffusion and dispersion parameters. For homologous association, parameters may be fitted to surrogates of molecular weights close to that of monomer and dimer. Optimized values of these parameters are not altered during fitting of interacting mixtures.

Step 2. Kinetic rate parameters governing interaction between two species are systematically varied to optimize correspondence between simulated chromatogram and an experimental chromatogram. A range of kinetic rates will generate 'readonable' correlations between simulated and experimental chromatograms.

Step 3. The optimized parameters are used to predict elution patterns at other concentrations, higher and lower. Concentration ranges should be as broad as practicable over values that generate concentration dependent elution profiles.

Step 4. If significant deviations between experimental and calculated profiles are found, kinetic parameters are adjusted and the process returns to step 2.

Step 5. If good agreement between experimental and calculated elution profiles is obtained, then the process may be considered to be complete, or, parameters are varied to test the stability of convergence.

[..*Example(s) to be added at a later..date*....]

Caveats.

SCIMMS, in common with other methods that use size-exclusion chromatography to estimate affinities and kinetics of macromolecular interactions, implicitly assumes that this chromatography technique is experimentally passive; *i.e.*, provides an interpretable signal but does not modify the process under observation. Unfortunately, this assumption is not correct.

As discussed by Giddings (1970) the porous size-exclusion chromatography matrix assures that the apparent rate constants observed during chromatography can not be identical to those that govern ideal interactions, as in the test tube. This phenomenon results directly from the mechanism by which size-exclusion chromatography is acheived.

Solute molecules of small radius have a greater accessible volume within the chromatography radius than solute of larger radii. With more volume within which to diffuse, small molecules take longer to pass through the column. When considering interactions between molecules of different size, it is apparent that the column offers space to the smaller molecule into which the larger is not able to diffuse; *i.e.*, space in which no interaction can take place. In either homologous or heterologous interactions, it is clear that the complex has access to a smaller fraction of the matrix than either of the constituents. Thus, there exists zones into which either interactive solute can diffuse, but both cannot be there simultaneously.

In practice, the error that results from this effect probably will manifest itself as a small underestimation of affinity constant. The magnitude of the error will be a function of the kinetics of interaction and the sizes of interacting partners and complexes. Because of the systematic nature of the affinity modulation, it is unlikely that this source of error significantly jeopardizes conclusions drawn from most chromatography experiments. We do, however, plan to address this issue with a modified transport algorithm which will partition solutes into mobile and stationary zones.

Another source of error introduced by the chromatography technique arises from the possiblity of non-steric interactions between the solute molecule and the chromatography matrix. These interactions may be of ionic or hydrophobic origin, depending upon the structural features of the solute molecule and the chemical composition of the matrix. Such interactions can usually be revealed as variation in elution position as a function of salt concentration in the buffer; increased salt will screen ionic interactions leading to ealier elution and will enhance hydrophobic interactons resulting in retarded elution.

References

The following listing includes all papers cited in this document. In addition, numerous papers that are also relevant to the application of size-exclusion chromatography methods are listed. This listing is not all inclusive.

Ackers, G.K. Molecular exclusion and restricted diffusion processes in molecular sieve chromatography. Biochemistry 3: 723–730, 1964.

Ackers, G.K. Molecular sieve methods of analysis. In The Proteins, 3rd edition, pp 1–94,. H. Neurath and R.L. Hill, eds. Academic Press, New York, 1975.

Ackers, G.K. and T.E. Thompson. Determination of stoichiometry and equilibrium constants for reversibly associating systems by molecular sieve chromatography. Proc. Natl. Acad. Sci, USA 53: 342–349, 1965.

Andrews, P. Estimation of the molecular weights of proteins by Sephadex gel-filtration. Biochem. J. 91: 222–233, 1964.

Andrews, P.R. and P.D. Jeffrey. Calculated sedimentation ratios for assemblies of two, three, four, and five spatially equivalent protomers. Biophys. Chem. 11: 49–59, 1980.

Arakawa, T. Thermodynamic analysis of the effects of concentrated salts on protein interaction with hydrophobic and polysaccharide columns. Arch. Bioch. Bioph. 248: 101–105, 1986.

Avila, L.Z., Y.-H. Chu, E.C. Blossey, and G. M. Whitesides. Use of affinity capillary electrophoresis to determine kinetic and equiibrium constants for binding of arylsulfonamides to bonvine carbonic anhydrase. J. Med. Chem. 36: 126–133, 1993.

Azuma, T., K. Hamaguchi, and S. Migita. Interactions between immunoglobulin polypeptide chains. J. Biochem. 76: 685–693, 1974.

Baghurst, P.A., L.W. Nichol, A.G. Ogston, and D.J. Winzor. Quantitative interpretation of concentration-dependent migration in gel chromatography of reversibly polymerizing solutes. Biochem. J. 147: 575–583, 1975.

Baudin-Chich V., M. Marden, and H. Wajcman. Investigation of the tetramer-dimer equilibrium in haemoglobin solutions by high-performance size-exclusion chromatography on a diol column. J. Chromatog. 437: 193–201, 1988.

Brown B.B. and J. K. Zimmerman. Active enzyme gel chromatography: II. Computer simulations. Bioph. Chem. 5: 351–357, 1976.

Brumbaugh, E.E. and G.K. Ackers. Molecular sieve studies of interacting protein systems. VII. Direct optical scanning method for ligand-macromolecule binding studies. Analyt. Biochem. 41: 543–559, 1971.

Brumbaugh, E.E. and G.K. Ackers. Molecular sieve studies of interacting protein systems. III. Measurement of solute partitioning by direct ultraviolet scanning of gel columns. J. Biol. Chem. 243: 6315–6324, 1968.

Brumbaugh, E.E., E.E. Saffen, and P.W. Chun. Scanning molecular sieve chromatography of interacting protein systems. II. Determination of large zone transport parameters by the difference profile method at low solute concentration. Biophys. Chem. 9: 299–311, 1979.

Cann, J.R., A.G. Appu Rao, and D.J. Winzor. Numerical and experimental demonstrations of the need for caution in the use of zonal gel chromatography for characterizing ligand interactions with small acceptors. Arch. Biochem. Biophys. 270: 173–183, 1989.

Cann, J.R. and N.D. Hinman. Hummel–Dreyer gel chromatographic procedure as applied to ligand–mediated association. Biochemistry 15: 4614–4622, 1976.

Cann, J.R., E.J. York, J.M. Stewart, J.C. Vera, and R.B. Maccioni. Small zone gel chroma-tography of interacting systems: theoretical and experimental evaluation of elution profiles for kinetically controlled macromolecule–ligand reactions. Analyt. Biochem. 175: 462–473, 1988.

Cann, J.R. and D.J. Winzor. Frontal gel chromat-ography of interacting systems: theoretical and experimental evaluation of the shapes of elution profiles for systems of the type A + B <=> C. Arch. Biochem. Biophys. 256: 78–89, 1987.

Chiancone E. and D. Winzor. Subunit-exchange chromatography of self-associating proteins: a quantitative reappraisal. Analyt. Biochem. 158: 211–216, 1986.

Chun P.W. and M.C.K. Yang. Scanning molecular sieve chromatography of interacting protein systems. Simulation of large zone behavior for self-associating solutes undergoing rapid chemical equilibration under kinetic control. Biophy. Chem. 7: 347–366, 1978.

Chun, P.W. and M.C.K Yang. Scanning molecular sieve chromatography of interacting protein systems. III. Effect of kinetic parameters on the large zone boundary profiles for local equlibration between mobile and stationary phases. Biophys. Chem. 9: 313–328, 1979.

Chun, P.W., E.E. Saffen, and J.Q. Oeswein. Thermodynamic compensation process in interacting protein systems: Definition of thermodynamic compensatory temperature. Biophys. Chem. 10: 129–141, 1979.

Cox, D.J. Computer simulation of sedimentation in the ultracentrifuge. I. Diffusion. Arch. Biochem. Biophys. 112: 249–258, 1965.

Cox, D.J. Computer simulation of sedimentation in the ultracentrifuge. II. Concentration-independent sedimentation. Arch. Biochem. Biophys. 112: 259–266, 1965.

Cox, D.J. Computer simulation of sedimentation in the ultracentrifuge. III. Concentration- dependent sedimentation. Arch. Biochem. Biophys. 119: 230-239, 1967.

Cox, D.J. Computer simulation of sedimentation in the ultracentrifuge. IV. Velocity sedimentation of self-associating solutes. Arch. Biochem. Biophys. 129: 106–123, 1969.

Cox, D.J. Computer simulation of sedimentation in the ultracentrifuge. V. Ideal and non-ideal monomer-trimer systems Arch. Biochem. Biophys. 142: 514–526, 1971.

Cox, D.J. Calculation of simulated sedimentation velocity profiles for self-associating solutes. Meth. Enzymol. 48: 212–242, 1978.

Cox, D.J. and R.S. Dale. Simulation of transport experiments for interacting systems. In Proteins-Proteins Interactions. C. Frieden and L.W. Nichol, editors. John Wiley and Sons, New York. pp 173–212, 1981.

Crawford, G.D., L. Correa, and P.M. Salvaterra. Interaction of monoclonal antibodies with mammalian choline acetyltransferase. Proc. Natl. Acad. Sci., USA 79: 7031–7035, 1982.

DePalo, E., R. Gatti, N. Sicolo, and C. dePalo. Human growth hormone association and binding study in vitro: high performance size exclusion chromatography and radioimmunoassay-measured levels in plasma of normal and acromegalic subjects. Clin. Physiol. Biochem. 8: 211–220, 1990.

Dickerman, J., B. Clevinger, and B. Friedenson. Loss of an individual idiotype on chemical modification. A strategy for assigning idiotypic determinants. J. Exp. Med. 153: 1275–1285, 1981.

Dishon, M., G.H. Weiss, and D.A. Yphantis. Numerical solutions of the Lamm equation. I. Numerical procedure. Biopolymers 4: 449–455, 1966.

Dishon, M., G.H. Weiss, and D.A. Yphantis. Numerical solutions of the Lamm equation. II. Equilibrium sedimentation. Biopolymers 4: 457–468., 1966.

Eisenberg, D. and A.D. McLachlan. Solvation energy in protein folding and binding. Nature 319: 199–203, 1986.

Endo, S., H. Hayashi, and A. Wada. Affinity chromatography without immobilized ligands: A new method for studying macromolecular interactions using high-performance liquid chromatography. Analyt. Biochem. 124: 372_379, 1982.

Endo, S. and A. Wada. Theoretical and experimental studies on zone-interferance chromatography as a new method for determining macromolecular kinetic constants. Biophys. Chem. 18: 291–301, 1983.

Fassina, G., H.E. Swaisgood, and I.M. Chaiken. Quantitative high-performance affinity chromatography: evaluation of use for analyzing peptide and protein interactions. J. Chromatog. 376: 87–93, 1986.

Fex, G, P. Albertsson, and B. Hansson. Interaction between prealbumin and retinol-binding protein studied by affintiy chromatography -- gel filtration -- and two-phase partition. Eur. J. Biochem. 99: 353–360, 1979.

Fitzgerald R. and H.E. Swaisgood. Binding of ions and hydrophobic probes to alpha-lactalbumin and kappa-casein as determined by analytical affinity chromatography. Arch. Bioch. Bioph. 268: 239–248, 1989.

Frankel, A.D., G.K. Ackers, and H.O. Smith. Measurement of DNA--protein equilibria using gel chromatography: application to the HinfI restriction endonuclease. Biochemistry 24: 3049–3054, 1985.

Ghrist, B.F.D., M.a. Stadalius, and L.R. Snyder. Predicting bandwidth in the high-performance liquid chromatographic separation of large biomolecules. I. Size-exclusion studies and the role of solute Stokes diameter versus particle pore diameter. J. Chromatog. 387: 1–19, 1987.

Giddings, J.C. Effect of membranes and other porous networks on the equilibrium and rate constants of macromolecular reactions. J. Phys. Chem. 74: 1368–1370, 1970.

Giddings, J.C. and H. Eyring. A molecular dynamic theory of chromatography. J. Phys. Chem. 50: 416–421, 1955.

Gilbert, G.A. Elution volume versus reciprocal elution volume in the interpretation of gel-filtration experiments. Nature 210: 299–300, 1966.

Gilbert, G.A. Layer technique in gel filtration for estimating differences in the degree of dissociation of closely related proteins. Nature 212: 296–297, 1966.

Gilbert, G.A. and R.C. L. Jenkins. Sedimentation and electrophoresis of interacting substances. II. Asymptotic boundary shape for two substances interacting reversibly. Proc. r. Soc. London, Ser. A 253: 420–437, 1959.

Gilbert, L.M. and G.A. Gilbert. Molecular transport of reversibly reacting systems: asymptotic boundary profiles in sedimentation, electrophoresis, and chromatography. Meth. Enzymol. 48: 195–212, 1978.

Gorbunov, A.A., A.Y. Lukyanov, V.A. Pasechnik, and A.V. Vakhrushev. Computer simulation of protein adsorption and chromatography. J.

Chromat. 365: 205–212, 1986.

Halvorson, H.R. and G.K. Ackers. Molecular sieve studies of interacting protein systems. XI. Isomerizing solutes. J. Biol. Chem. 249: 967–973, 1974.

Hamielec A and M. Styring. Recent advances in the characterization and analysis of polymers and polymer particles by size exclusion chromatography. Pure & Appl. Chem. 57; 955–970, 1985.

Hayashi, Y., H. Matsui, and T. Takagi. Membrane protein molecular weight determined by low-angle laser light-scattering photometry coupled with high-performance gel chromatography. Meth. Enzymol. 172: 514–528, 1989.

Hayashi Y., K. Mimura, H. Matsui, and T. Takagi. Minimum enzyme unit for Na+/K+ - ATPase is the alpha/beta-protomer. Determination by low-angle laser light scattering photometry coupled with high-performance gel chromatography for substantially simultaneous measurement of ATPase activity and molecular weight. Biochim. Biophys. Acta. 983: 217–229, 1989.

Hayashi, Y., T. Takagi, S. Maezawa, and H. Matsui. Molecular weights of alpha-beta-protomeric and oligomeric units of soluble (Na+,K+)-ATPase determined by low-angle laser light scattering after high-performance gel chromatography. Biochim. Biophys. Acta. 748: 153–167, 1983.

Hummel, J.P. and W.J. Dreyer. Measurement of protein-binding phenomena by gel filtration. Biochim. Biophys. Acta 63: 530–532, 1962.

Jones, D.H., A.J. McMillan, A.R. Fersht, and G. Winter. Reversible dissociation of dimeric tyrosyl-tRNA synthetase by mutagenesis at the subunit interface. Biochemistry 24: 5852–5857, 1985.

Liu, Y.C. and E. Stellwagen. Zonal chromatographic analysis of the interaction of alcohol dehydrogenase with blue-sepharose. J. Chromat.og. 376: 149–155, 1986.

Kegeles, G. and J.R. Cann. Kinetically controlled mass transport of associating-dissociating macromolecules. Meth. Enzymol. 48: 248–270, 1978.

Mahieu, J–P, B. Sebille, C.T. Craescu, M–D Rhoda and Y. Beuzard. Determination of the dissociation constant of oligomeric proteins by size-exclusion high-performance liquid chromatography: application to human haemoglobin. J. Chromatog. 327: 313–325, 1985.

Maltsev, V.G., T.M. Zimina, B.G. Belenkii, and O.I. Kurenbin. Microbore column exclusion chromatographic method for studying protein association and its relation with enzymatic activity. J. Chromatog. 273: 95–105, 1983.

McPerson D.D. and J.M. Pezzuto. Interaction of 9-aminoacridin, ethidium bromide and harman with DNA characterized by size-exclusion high-performance liquid chromatography. J. Chromat. 281: 348–354, 1983.

Meng, Q.C, Y.-F. Chen, L.J. DeLucas, and S. Oparil. Effect of steric exclusion on the separation of proteins by hydrophilic size-exclusion chromatography. J. Chromatog. 445: 29–36, 1988.

Mitchell, R.M. The spatial distribution of moving macromolecules undergoing isomerization. Biopolymers 15: 1717–1739.

Murao, S.-I, F.J. Stevens, A. Ito, and E. Huberman. Myeloperoxidase: A myeloid cell nuclear antigen with DNA-binding properties. Proc. Natl. Acad. Sci, USA 85: 1232–1236, 1988.

Myatt, E.A., P.T.P. Kaumaya, and F.J. Stevens. Applications of size-exclusion HPLC in the analysis of peptide epitopes. BioChromatography 4: 282–289, 1989.

Myatt, E.A., F.J. Stevens, and P.B. Sigler. Effects of pH and calcium ion on self-association properties of two dimeric phopholipases A2. J. Biol. Chem. 266: 16331–16335, 1991.

Nichol, L.W., M. Janado, and D. Winzor. The origin and consequences of concentration dependence in gel chromatography. Biochem. J. 133: 15–22, 1973.

Nichol, L.W. and A.G. Ogston. A generalized approach to the description of interaction boundaries in migrating systems. Proc. R. Soc. London B163: 343–368, 1965.

Nichol, L.W., A.G. Ogston, and D.J. Winzor. Evaluation of gel filtration data on systems interacting chemically and physically. Arch. Biochem. Biophys. 121: 517–521, 1967.

Nichol, L.W., A.G. Ogston, and B.N. Preston. The equilibrium sedimentation of hyaluronic acid and of two synthetic polymers. Biochem. J. 102: 407–416, 1979.

Nichol, L.W., A.G. Ogston, and P.R. Wills. Effect of inert polymers on protein self-association. FEBS Letts. 126: 18–20, 1981.

Nichol, L.W., E.A. Owen, and D.J. Winzor. A macromolecular shape function based on sedimentation velocity parameters. Arch. Biochem. Biophys. 236: 338–341, 1985.

Nichol, L.W., M.J. Sculley, L.D. Ward, and D.J. Winzor. Effects of thermodynamic non-ideality in kinetic studies. Arch. Biochem. Biophysl 222: 574–581, 1983.

Nichol, L.W., R.J. Siezen and D.J. Winzor. The study of multiple polymerization equilibria by glass bead exclusion chromatography with allowance for thermodynamic non-ideality effects. Biophys. Chem. 9: 47–55, 1978.

Nichol, L.W., R.J. Siezen, and D.J. Winzor. Chromatographic evidence of the self-association of oxyhemoglobin in concentrated solutions: its biological implications. Biophys. Chem. 10: 17–26, 1979.

Nimmo, I.A. and A. Bauermeister. A theoretical analysis of the use of zonal gel filtration in the detection and purification of protein-ligand complexes. Biochem. J. 169: 437–440, 1978.

Ogston, A.G. and D.J. Winzor. Treatment of thermodynamic nonideality in equilibrium studies on associating solutes. J. Phys. Chem. 79: 2496–2500, 1975.

Oshima, G., H. Uchiyama, and K. Nagasawa. 1981. A new method for determining the dissociation constant between macromolecules by gel permation. Analyt. Biochem. 111: 366–371, 1981.

Patience, R.L. and L.H. Rees. Comparison by gel filtration chromatography and reversed-phase high-performance liquid chromatography of the immunoreactive growth hormone composition of a human pituitary extract. J. Chromatog. 324: 385_393, 1985.

Porath, J. Molecular-sieving and non-ionic adsorption in polysaccharide gels. Biochem. Soc. Transact. 7: 1197–1222, 1979.

Saffen, E.E. and P.W. Chun. Scanning molecular sieve chromatography of interacting protein systems .IV. The difference profile method as applied to the Gibbs-Duhem expression in the analysis of the dimer-tetramer equilibria of oxyhemoglobin A. Biophys. Chem. 9: 329–344, 1979.

Short, M.T., F.A. Westholm, M. Schiffer, and F.J. Stevens. Comparison of chromatographic characteristics of a series of homologous Bence Jones proteins during size-exclusion chromatography by high-performace liquid chromatography and by Sephadex. J. Chromatog. 323: 418–423, 1985.

hypervariable region. Proc. Natl. Acad. Sci., USA 77: 1144–1148, 1980.

Siegel, R.C. and V.N. Schumaker. Measurement of the association constants of the complexes formed between intact C1q or pepsin-treated C1q stalks and the unactivated or activated C1r2C1s2 tetramers. Molec. Immunol. 20: 53–66, 1983.

Stadalius, M.A., B.F.D. Ghrist, and L.R. Snyder. Predicting bandwidth in the high-performance liquid chromatographic separation of large biomolecules. II. A general model for the four common high-performance liquid chromatography methods. J. Chromatog. 387: 21–40, 1987.

Stevens, F.J. Analysis of protein–protein interaction by simulation of small-zone size exclusion chromatography: application to an antibody–antigen association. Biochemistry, 25: 981–993, 1986.

Stevens, F.J. Size-exclusion chromatography system for macromolecular interaction analysis. U.S. Patent # 4,762,617. 1988.

Stevens, F.J. Analysis of protein–protein interaction by simulation of small-zone size-exclusion chromatography: stochastic formulation of kinetic rate contributions to observed high-performance liquid chromatography elution characteristics. Biophys. J. 55:1155– 1167, 1989.

Stevens, F.J. Size-exclusion high-performance liquid chromatography in analysis of protein and peptide epitopes. Meth. Enzymol. 178: 107–130, 1989.

Stevens, F.J., W.E. Carperos, W.J. Monafo, and N.S. Greenspan. Size-exclusion HPLC analysis of epitopes. J. Immunol. Meth. 108: 271–278, 1988.

Stevens, F.J. and M. Schiffer. Computer simulation of protein self-association during small-zone gel filtration Biochem. J. 195: 213–219, 1981.

Stevens, F.J., F.A. Westholm, A. Solomon, and M. Schiffer. Self–association of human immunoglobulin light chains: role of the third

Stevens, F.J., D.A. LeBuis, W.J. Eisler, and C.F. Ainsowrth. Macromolecular interactions: application of microcomputer-controlled high-speed size-exclusion chromatography. Liq. Chrom. Gas Chrom. 4: 340–348, 1986.

Sullivan, B. and A. Riggs. The subunit dissociation properties of turtle hemoglobins. Biochim. Biophys. Acta 140: 274–283, 1967.

Swaisgood H.E. and I.M. Chaiken. Analytical high-performance affinity chromatography: Evaluation by studies of neurophysin self-association and neurophysin-peptide hormone interaction using glass matrices. Biochemistry 25: 4148–4155, 1986.

Tellam, R. and D.J. Winzor. Concentration-dependent migration in gel chromatography of reversibly polymerizing solutes: the osmotic behavior of polyacrylamide gels. Biophys. Chem. 12: 299–306, 1980.

Tojo, H., K. Horiike, K. Shiga, Y. Nishina , M. Nozaki, H. Watari, and T. Yamano. Gel chromtographic evidence for the participation of the higher polymers in the self-association system of a flavoenzyme D-amino acid oxidase. J. Biochem. 95: 1–6, 1984.

Tojo, H., K. Horiike, K. Shiga, Y. Nishina, H. Watari, and T. Yamano. Self-association mode of a flavoenzyme D-amino acid oxidase from hog kidney. I. Analysis of apparent weight-average molecular weight data for the apoenzyme in terms of models. J. Biol. Chem. 260: 12607–12614, 1985.

Tojo, H., K. Horiike, K. Shiga, Y. Nishina, H. Watari, and T. Yamano. Self-association mode of a flavoenzyme D-amino acid oxidase from hog kidney. II. Stoichiometry of holoenzyme association and energetics of subunit association. J. Biol. Chem. 260: 12615–12621, 1985.

Vilenchik L.Z., O.I. Kurenbin, Y.Y. Gotlib, and B.G. Belenkii. Gel-penetrating chromatography of interacting multicomponent systems. I. Study of the isomerization of proteins by the method of gel-penetrating chromatography. 1. Theory of method. Biofizika 22: 582–588, 1977.

Vilsen, B. and J.P. Andersen. Use of a small TSK GSW high-performance liquid chromatographic column for large-zone chromatographic studies of monomer-oligomer equilibria of membrane proteins. J. Chromatog. 442: 229–236, 1988.

Weiss, G.H. and G.K. Ackers. Magnitude of a finite equilibration effect in analytical gel chromatography. Biopolymers 11: 2125–2130, 1972.

Willey, K.P. Simple and complex antibody reactions in radioimmunassay and the prediction of assay characteristics. J. Immunol. Meth. 84: 343–358, 1985.

Winzor, D.J. and H. A. Scheraga. Studies of chemically reacting systems on Sephadex. I. Chromatographic demonstration of the Gilbert theory. 2: 1263–1267, 1963.

Zimina, T.M., V.G. Maltsev, and B.G. Belenkii. Study of protein association and micelle formation in surfactants by microcolumn exclusion chromatography. J. High. Res. Chrom & Chrom. Communications. 9: 111–115, 1986.

Zimmerman, J.K. Kinetically controlled association-dissociation reactions in gel chromatography. Biochemistry 13: 384–389, 1974.

Zimmerman, J.K. Kinetic control of three-species association reactions in gel chromatography. Biophys. Chem. 3: 339–344, 1975.

Zimmerman, J.K. Time difference scanning gel chromatography: computer simulations. Biophys. Chem. 11: 173–181, 1980.

Zimmerman, J.K. and G.K. Ackers. Molecular sieve studies of interacting proteins systems. VI. Effects of axial dispersion on boundary profiles of associating macromolecules. J. Biol. Chem. 246: 1078–1087, 1971.

Zimmerman, J.K. and G.K. Ackers. Molecular sieve studies of interacting proteins systems. X. Behavior of small zone profiles for reversibly self-associating solutes. J. Biol. Chem. 246: 7289–7292, 1971.

Zimmerman, J.K., D.J. Cox, and G.K. Ackers. Molecular sieve studies of interacting protein systems. IX. Reaction boundary profiles for monomer-n-mer systems: comparison with sedimentation. J. Biol. Chem. 246: 4242–4250, 1971.